



Published in final edited form as:

J Biomol Screen. 2016 July ; 21(6): 643–652. doi:10.1177/1087057116629381.

Identification of HDAC inhibitors using a cell-based HDAC I/II assay

Chia-Wen Hsu, David Shou, Ruili Huang, Thai Khuc, Sheng Dai, Wei Zheng, Carleen Klumpp-Thomas, and Menghang Xia*

National Center for Advancing Translational Sciences, Bethesda, MD 20892, USA

Abstract

Histone deacetylases (HDACs) are a class of epigenetic enzymes that regulate gene expression by histone deacetylation. Altered HDAC function has been linked to cancer and neurodegenerative diseases, making HDACs popular therapeutic targets. In this study, we describe a screening approach for identification of compounds that inhibit endogenous class I and II HDACs. A homogeneous, luminogenic HDAC I/II assay was optimized in a 1536-well plate format in several human cell lines including HCT116 and human neural stem cells. The assay confirmed 37 known HDAC inhibitors from two libraries of known epigenetics-active compounds. Using the assay, we identified a group of potential HDAC inhibitors by screening the NCATS Pharmaceutical Collection (NPC) of 2,527 small molecule drugs. The selected compounds showed similar HDAC I/II inhibitory potency and efficacy values in both HCT116 and neural stem cells. Several previously unidentified HDAC inhibitors were further evaluated and profiled for their selectivity against a panel of ten HDAC I/II isoforms using fluorogenic HDAC biochemical assays. In summary, our results show that several novel HDAC inhibitors including nafamostat and piceatannol have been identified using the HDAC I/II cell-based assay, and multiple cell types have been validated for high-throughput screening of large chemical libraries.

Keywords

Histone deacetylase; epigenetics; cancer; neurodegenerative disease; qHTS

Introduction

Epigenetic aberrations contribute substantially to the onset and progression of human disease. A group of enzymes called histone deacetylases (HDACs) are capable of introducing epigenetic modifications¹. The major function of HDACs is to remove an acetyl group from a ϵ -N-acetyl lysine residue on a histone, causing an increase in positive charges at the residue and enhancing the binding ability of histones to negatively charged deoxyribonucleic acid (DNA) molecules². HDACs also regulate gene expression by deacetylating non-histone proteins such as tubulin and several transcription factors (e.g.,

*Address correspondence to: Menghang Xia, Ph.D., National Institutes of Health, National Center for Advancing Translational Sciences, 9800 Medical Center Drive, Bethesda, MD 20892, Phone: 301-217-5718, mxia@mail.nih.gov.

Declaration of Conflicting Interests

The author(s) declared no potential conflicts of interest with respect to the research, authorship, and/or publication of this article.

p53, CREB, and NF- κ B). Based on sequence similarity to yeast HDAC homologs, the HDAC family containing eighteen enzymes is categorized into four classes— I, II, III, and IV. Class I and II HDACs include HDAC1, HDAC2, HDAC3, HDAC4, HDAC5, HDAC6, HDAC7, HDAC8, HDAC9, and HDAC10. Class III HDACs, or sirtuins (SIRT), contain seven isoforms in mammals. Class IV HDACs only have one isoform, HDAC11. Class I and II HDACs have similar substrate specificity and sensitivity to trichostatin A inhibition³. Class III HDACs require nicotinamide adenine dinucleotide (NAD) coenzymes for activation and class II HDACs can be categorized into subgroups of class IIa and class IIb enzymes². HDAC isoforms exert distinct functions in various tissues; therefore, altered HDAC functions have been implicated in cancer and neurological disorders⁴. Inhibition of class I HDACs, including HDAC1, HDAC2, and HDAC3, has been shown to suppress tumor differentiation and transformation in promyelocytic leukemia (PML)⁵. For example, the commonly-used control compound trichostatin A and the FDA-approved drug vorinostat (SAHA), first discovered as anti-cancer agents, were later characterized as class I and II HDAC inhibitors⁴. One of the class I HDACs(HDAC2), and three of the class II HDACs(HDAC4, HDAC5, and HDAC9), regulate the development and function of the brain and other neurological systems, playing an important role in Alzheimer's disease and Parkinson's disease. Due to the diverse physiological function and disease relevance of HDACs, several isoform-specific HDAC inhibitors are under pre-clinical development and clinical trials, such as the HDAC3 inhibitor, RGFP966, for the treatment of cancer and neurological diseases, and the HDAC6 inhibitor, tubastatin A, for the treatment of neurodegeneration, demonstrating that HDACs are important therapeutic targets for further drug development.

Conducting high-throughput screening (HTS) assays that measure HDAC activity in biochemical or cell-based formats is the initial step toward identifying HDAC modulators that may later be developed into drugs for the treatment of HDAC-relevant diseases. Several HTS-compatible HDAC enzyme activity assays based on bioluminogenic reaction⁶, fluorescence anisotropy⁷, fluorescence lifetime⁷, fluorescence polarization (FP)⁸, fluorescence resonance energy transfer (FRET)⁹, and fluorogenic reaction¹⁰ have been employed in previous studies. Furthermore, a panel of isoform-specific and cell-based HDAC assays were recently developed in 96- and 384-well plate formats through coupling of enzyme-linked immunosorbent assays (ELISAs) for each HDAC isoform with a generic bioluminescence reaction¹¹. In this study, we describe a cell-based screening approach for rapid identification of compounds that potentially inhibit class I and II HDACs. A homogenous, luminogenic HDAC I/II assay was first optimized in several human cancer cell lines and human neural stem cells in 1536-well plate formats. The assay was validated by using known epigenetic compound libraries and by profiling the NCATS Pharmaceutical Collection (NPC) of approved and investigational drugs. The identified potential HDAC inhibitors were further confirmed by fluorogenic HDAC isoform-specific biochemical assays. Our results show that the HDAC I/II luminescent assays can detect endogenous HDAC I/II activities in various cell backgrounds and can be used for high-throughput screening of large chemical libraries.

Material and Methods

Reagents

Four cell lines (human colon cancer cell line HCT116, human embryonic kidney cell line HEK293, human liver cancer cell line HepG2, and human B lymphoma cell line SU-DHL-6), fetal bovine serum (FBS), Eagle's Minimum Essential Medium (EMEM), and Roswell Park Memorial Institute (RPMI) 1640 medium were purchased from American Type Cell Collection (ATCC, Manassas, VA, USA). H9-derived human neural stem cells, defined FBS, trypsin-EDTA, fibronectin, basal fibroblast growth factor (bFGF), epidermal growth factor (EGF), KnockOut™ Dulbecco's Modified Eagle Medium (DMEM)/F12, and penicillin-streptomycin, StemPro® Neural Supplement were acquired from Life Technologies, Carlsbad, CA, USA. Chemicals and epigenetic compound libraries were purchased from Cayman Chemicals (Ann Arbor, MI), Santa Cruz Biotechnology (Dallas, TX, USA), SelleckChem (Houston, TX, USA), and Sigma-Aldrich (St. Louis, MO, USA). HDAC-Glo I/II and CellTiter-Glo reagents were purchased from Promega, Madison, WI. Fluorogenic assay kits for HDAC1, HDAC2, HDAC3, HDAC4, HDAC5, HDAC6, HDAC7, HDAC8, HDAC9, and HDAC10 were acquired from BPS Bioscience (San Diego, CA). White solid bottom 1536-well assay plates were purchased from Greiner Bio-One (Monroe, NC).

Cell Line and Cell Culture

HCT116 cells were cultured with RPMI-1640 Medium supplemented with 10% defined FBS, 100 U/mL penicillin and 100 µg/mL streptomycin. HEK 293 and HepG2 cells were cultured with EMEM supplemented with 10% FBS (ATCC), 100 U/mL penicillin, and 100 µg/mL streptomycin. SU-DHL-6 cells were cultured in RPMI-1640 medium supplemented with 10% FBS (ATCC), 100 U/mL penicillin, and 100 µg/mL streptomycin. Human neural stem cells in CELLstart-coated flasks were cultured in KnockOut™ DMEM/F12 medium supplemented with 2mM GlutaMAX™, StemPro® Neural Supplement, and 20 ng/mL EGF and bFGF. All cell lines were cultured in a 37°C humidified incubator with 5% CO₂. HCT116, HEK293, and HepG2 cells were passaged at 70-90% confluence with 0.25%, 0.05% and 0.25% trypsin-EDTA, respectively. SU-DHL-6 cells were maintained at 2×10^6 cells per mL by supplying fresh medium every 3 to 4 days.

HDAC-Glo I/II and Cell Viability Assays

HCT116, HEK293, HepG2, and SU-DHL-6 cells were seeded into 1536-well white solid bottom assay plates at desired cell densities in 5 µL medium using a microfluidic reagent dispenser (BioRAPTR FRD, Beckman Coulter, Indianapolis, IN). Before plating 5 µL of human neural stem cells into each well, assay plates were pre-coated with 5 µL of 10 µg/mL fibronectin in culture medium at 37°C for one hour and the coating solution was removed by centrifuging the inverted plates. Cells were settled overnight in a cell incubator at 37°C, 5% CO₂, followed by addition of 23 nL of compound solution on a pintool workstation (Kalypsys, San Diego, CA). After compound incubation for indicated period at 37°C/5% CO₂, 5 µL of HDAC-Glo was dispensed using BioRAPTR FRD. To measure cell viability, 5 µL of CellTiter-Glo Cell Viability reagent was added to each well in a separate assay plate

using BioRAPTR FRD. The luminescence signals of HDAC-Glo and CellTiter-Glo assays were measured on a ViewLux plate reader (Perkin-Elmer, Shelton, CT).

Compound Screening and Data Analysis

For primary screening of the NPC, 1500 HCT116 cells in 5 μL assay medium were seeded into each well using a 8-tip Multidrop dispenser (Thermo Scientific, Waltham, MA). Cells were plated overnight in a humidified incubator at 37°C, 5%CO₂, followed by an online workflow of compound addition, assay plate incubation, reagent addition, and plate reading on a robotic quantitative high-throughput screening (qHTS) platform (Kalypsys, San Diego, CA). For validation and confirmation studies, HCT116, HEK293, and human neural stem cells were seeded at 1500, 1500, and 4000 cells per well, respectively, using BioRAPTR FRD. All wells were added with 23 nL of test compounds or DMSO and incubated at 37°C, 5%CO₂ for 1 hour. HDAC-Glo and CellTiter-Glo assays were conducted accordingly. Analysis of the qHTS data was performed as follows. First, raw plate reads containing individual titration points were normalized relative to the controls (i.e., DMSO as 0% inhibition in HDAC activity or cytotoxicity, trichostatin A (TSA) as 100% HDAC inhibition, and tetraoctylammonium bromide (TOAB) as 100% cytotoxicity) using the following formula: % activity = $((V_{\text{compound}} - V_{\text{DMSO}})/(V_{\text{pos}} - V_{\text{DMSO}})) \times 100$, where V_{compound} , V_{pos} , and V_{DMSO} denote for the median value of the compound wells, the positive control wells, and the DMSO-only wells respectively. The normalized plate reads were corrected with DMSO-only plates tested before and after the sample plates using a NCATS in-house pattern correction algorithm. The half-maximal inhibitory concentration (IC₅₀) and maximal response (efficacy) values were determined by fitting the concentration-response curves to a four-parameter Hill equation.

Fluorogenic Isoform-specific HDAC Assays

The fluorogenic assays were performed at BPS Bioscience (San Diego, CA) for individual HDAC I/II enzymes (BPS Bioscience) using human recombinant enzymes and fluorogenic HDAC substrates¹²⁻¹⁴ (Suppl. Table S1). Briefly, a 50 μL buffer (50 mM Tris-HCl, pH7.4, 137 mM NaCl, 2.7 mM KCl, 0.05% Tween-20, and 5 $\mu\text{g}/\text{mL}$ BSA) mixture containing the human recombinant HDAC enzyme isoform test compound and the corresponding HDAC substrate was added into a black 96-well assay plate. The reaction in each well was incubated at 37°C for 30 minutes, followed by adding 50 μL of HDAC Developer reagent and incubated at room temperature for an additional 20 minutes. Fluorescence intensity of the assay plates was measured on an Infinite M100 microplate reader (Tecan, San Jose, CA) using an excitation wavelength of 360 nm and an emission wavelength of 460 nm for all compounds at 20 μM and concentration-response curves of non-blue fluorescent compounds and an excitation wavelength of 490 nm and an emission wavelength of 530 nm for blue fluorescent compounds (e.g., concentration-response curves for nafamostat). The fluorescence intensity data was analyzed using Prism (GraphPad Software, La Jolla, CA). The DMSO controls (F_t) and enzyme-free controls (F_b) were defined as 100% and 0% HDAC activity respectively. The percent activity of each compound was calculated as $(F - F_b)/(F_t - F_b)$, where F represents the fluorescence intensity value at the specified compound concentration.

Results

Optimization of Cell-based HDAC-Glo I/II Assays

The HDAC-Glo I/II assay was optimized in 1536-well plate formats by measuring the inhibitory effect of trichostatin A on endogenous HDAC I/II activities in a panel of five human cell lines, SU-DHL-6, HCT116, HEK293, HepG2, and human neural stem cells (hNSCs) (**Figure 1A**). The assay uses a cell permeable HDAC I/II substrate that can be converted into a luciferase substrate upon deacetylation by endogenous HDACs, therefore no wash steps are needed in the cell-based HDAC-Glo I/II assays. Compared to HEK293 cells, the HCT116, HepG2, SU-DHL-6 and hNSCs showed higher basal activity levels of HDAC I/II enzymes at their optimal cell densities. The time course of one hour treatment for trichostatin A in HCT116 cells had the most potent activity ($IC_{50} = 0.05 \pm 0.03 \mu\text{M}$) compared to other time points for the HDAC-Glo I/II assay (**Figure 1B**). Based on the signal to background ratio (S/B), Z' factor, and IC_{50} values of the five cell lines (Suppl. **Table S2**), the HCT116 cell line and a compound incubation time of one hour were selected for the following assay validation and compound primary screening.

Validation of HDAC-Glo I/II Assay with Epigenetics Libraries

The HDAC-Glo I/II assay was evaluated using two epigenetic chemical libraries, Cayman (<https://www.caymanchem.com/app/template/Product.vm/catalog/11076>) and the SelleckChem (<http://www.selleckchem.com/screening/epigenetics-compound-library.html>) chemical collections. Each compound was tested at multiple concentrations ranging from 0.7 nM-46 μM in HCT116 and HEK293 cells. Out of the 22 known HDAC I/II inhibitors from the Cayman collection, 18 compounds showed HDAC I/II inhibitory activities, whereas 26 out of the 31 known HDAC I/II inhibitors in the SelleckChem chemical collection showed assay activities as shown in Supplemental **Table S3**. In addition to hydroxamate-based HDAC inhibitors (e.g., trichostatin A and vorinostat), the assay identified several non-hydroxamate-based HDAC inhibitors such as apicidin, benzamides (e.g., entinostat, chidamide, and RGFP966), a cyclic peptide (HC Toxin), and a stilbenoid (resveratrol). Compared to trichostatin A and vorinostat that greatly inhibited HDAC-Glo I/II activity, inhibitors of class III HDACs (SIRT) such as selisistat (EX-527) were inactive (**Figure 1C**). Piceatannol, a resveratrol analog, inhibited HDAC-Glo activity in HCT116 and HEK293 cell lines with IC_{50} values of $4.88 \pm 0.33 \mu\text{M}$ and $5.22 \pm 2.61 \mu\text{M}$, respectively. The assay also identified isoliquiritigenin as a novel HDAC inhibitor with IC_{50} values of $1.60 \pm 0.10 \mu\text{M}$ in HCT116 cells and $0.92 \pm 0.57 \mu\text{M}$ in HEK293 cells.

qHTS of NPC for HDAC I/II Inhibitors

The HDAC-Glo I/II assay using HCT116 cells identified 43 (1.7%) active compounds from the NPC library based on potency ($IC_{50} < 10 \mu\text{M}$) and efficacy (> 70%). Each compound was tested at eight concentrations ranging from 0.6 nM to 92 μM . The online screen of HDAC assay yielded a signal-to-background (S/B) ratio of 5.34 ± 0.56 fold, a coefficient of variation (CV) of $2.83 \pm 0.49 \%$, and Z' factor of 0.84 ± 0.19 . The positive control compound trichostatin A had an IC_{50} value of $0.16 \pm 0.03 \mu\text{M}$. The assay identified both of the two known HDAC inhibitors—resveratrol ($IC_{50} = 2.66 \mu\text{M}$) and vorinostat ($IC_{50} = 0.67 \mu\text{M}$)—from the NPC library. Nafamostat was the most potent hit ($IC_{50} = 0.07 \mu\text{M}$)

identified from the primary screening. Both nafamostat and its analog camostat ($IC_{50} = 0.60 \mu\text{M}$) reduced HDAC-Glo signals at submicromolar concentrations in HCT116 cells. Three benzimidazole-based compounds, including albendazole ($IC_{50} = 9.44 \mu\text{M}$), albendazole oxide ($IC_{50} = 3.76 \mu\text{M}$), and thiabendazole ($IC_{50} = 2.98 \mu\text{M}$), inhibited more than half of HDAC activity in the HDAC-Glo I/II HCT116 assay.

Confirmation of Identified HDAC Inhibitors

Fifty compounds, 7 from the epigenetic libraries and 43 from the NPC library, were cherry-picked and retested at 11 concentrations in HDAC-Glo I/II assay in HCT116 cells and human neural stem cells (hNSCs) (**Table 1**), yielding a confirmation rate of 94% (i.e., efficacy = 30%). The IC_{50} values of the top 20 potent compounds had a good correlation between HCT116 cells and hNSCs ($R^2=0.69$, **Table 1**). Camostat, nafamostat, piceatannol, and resveratrol completely inhibited HDAC-Glo I/II luminescence signals in hNSCs (**Figure 2**). Several compounds such as daniquidone, nitazoxanide and tenonitroazole were more potent in decreasing HDAC-Glo I/II signals than suppressing proliferation of HCT116 cells and hNSCs after one-hour incubation. Fifteen compounds, including four known HDAC inhibitors (resveratrol, trichostatin A, scriptaid, and vorinostat) and 11 HDAC-Glo I/II potential inhibitors, chosen based on potency and efficacy (i.e., $IC_{50} < 10 \mu\text{M}$ and 70% inhibition in the HDAC-Glo hNSC assay) from the cherry-pick confirmatory results, were prepared from powders and tested in the HDAC-Glo I/II assay with HCT116 cells (**Table 2**). All 15 compounds were confirmed to decrease HDAC-Glo I/II signals with less than three-fold changes in IC_{50} values.

Isoform Selectivity of Identified HDAC Inhibitors

The 15 potential inhibitors of HDACs were profiled at $20 \mu\text{M}$ for isoform selectivity with a panel of fluorogenic assays against ten class I and II HDAC isoforms (**Figure 3**). The known HDAC inhibitors such as trichostatin A, vorinostat and scriptaid inhibited activities of all isoforms, whereas resveratrol partially inhibited HDAC2 and HDAC6 at $20 \mu\text{M}$. Amlexanox inhibited more than half of enzyme activities of HDAC3, HDAC10, and HDAC11. Axitinib inhibited HDAC6 the most. In addition to HDAC3, isoliquiritigenin also weakly inhibited many class I and II HDAC enzymes at $20 \mu\text{M}$. Several potential HDAC inhibitors, including diphenyl isophthalate, ensulizole, febuxostat, and leflunomide selectively inhibited activity of HDAC3. Nafamostat had high basal fluorescence when excited at 360 nm, therefore red-shifted versions of fluorogenic assays were used to confirm its anti-HDAC activity. The results showed that nafamostat was more selective in inhibiting HDAC4, HDAC5, and HDAC8 than other HDAC isoforms (**Figure 4A**, **Figure 4B**, and Suppl. **Table S4**). Piceatannol inhibited HDAC activity by over 30% of HDAC1, HDAC2, HDAC5, HDAC7, HDAC8, and HDAC9 (**Figure 4C**, **Figure 4D**, and Suppl. **Table S4**).

Discussion

In this study we described a workflow for the identification of approved and investigational drugs that inhibit HDAC class I/II activity. The HDAC-Glo I/II assay was first developed as a biochemical, bioluminogenic HDAC activity assay that measures enzyme activity of individual class I and II HDAC isoforms⁶. We successfully optimized it to a cell-based assay

in 1536-well formats to measure endogenous HDAC I/II activity in five human cell lines including colon cancer HCT116 cells and human neural stem cells. All cell lines tested with the HDAC-Glo I/II assay yielded excellent S/B ratio, CV, and Z' factor values for high-throughput screening (HTS). The HDAC-Glo I/II assay in HCT116 and HEK239 cells identified several known HDAC class I and II inhibitors as shown in the validation results of the two epigenetic libraries, with a high correlation coefficient ($R^2 = 0.80$) in the IC_{50} values of the each cell line, respectively.

The HDAC-Glo I/II assay identified over 80% of known HDAC inhibitors from the Cayman Chemical's and the SelleckChem's epigenetic libraries. Most active compounds identified from the two libraries showed comparable potencies and efficacies in decreasing HDAC-Glo I/II signals in both HCT116 and HEK293 cells. Because the highest compound concentration tested in the HDAC-Glo I/II assay was 46 μ M for the epigenetic libraries, the three known HDAC inhibitors with milli-molar potencies—sodium butyrate, sodium phenylbutyrate, and valproic acid¹⁵—did not show concentration-dependent inhibition in the HCT116 and the HEK293 assays (Suppl. **Table S3**). Since many of the known HDAC inhibitors were discovered from biochemical HDAC assays with limited information regarding their ability to permeate cell membrane and directly inhibit HDAC activity in cellular environment, it will require other cell-based HDAC function assays such as western blotting of histone acetylation and tubulin acetylation to determine whether some of the known HDAC inhibitors were false negatives or true negatives in the cell-based HDAC-Glo I/II assay.

The qHTS results of the NPC library of approximately 2,500 compounds demonstrate the potential of applying the HDAC-Glo I/II assay in screening large numbers of compounds. The HDAC-Glo I/II HCT116 assay identified a group of compounds as potential inhibitors of HDAC class I and/or II enzymes. As shown in the cherry-pick confirmation assay data (**Table 1**), most of the HCT116-active compounds also reduced HDAC-Glo I/II signals in the human neural stem cells (hNSCs) without exerting apparent cytotoxicity to either cell lines after an one-hour compound treatment. All 15 compounds selected from the cherry-pick confirmation were also confirmed for their ability to decrease HDAC-Glo I/II signals in HCT116 cells (**Table 2**). Moreover the qHTS results showed that the cell-based HDAC-Glo assay can identify diverse chemical structural classes. In addition to hydroxamate-based HDAC inhibitors (e.g., trichostatin A and vorinostat), benzimidazoles (e.g., albendazole oxide and thiabendazole), guanidine acids (e.g., camostat and nafamostat), and stilbenes (e.g., piceatannol and resveratrol) also showed inhibited HDAC activity. It would be interesting to further characterize the structural-activity relationships (SARs) of these novel structural classes using the HDAC-Glo I/II assay and other secondary assays.

The fluorogenic HDAC biochemical assays were useful to confirm anti-HDAC activity and reveal isoform selectivity of the active compounds identified by the cell-based HDAC-Glo I/II assays. The fluorogenic assays were sensitive to the three known pan-HDAC inhibitors with submicromolar potencies—scriptaid, trichostatin A and vorinostat—as shown by over 80% inhibitions at 20 μ M against all class I and II HDAC enzymes. In general, the efficacy values at 20 μ M compound concentration were higher in the cell-based HDAC-Glo I/II assays than the isoform-specific biochemical assays, indicating potentially weaker IC_{50}

values against individual HDAC isoforms (**Table 2** and **Figure 3**). Several novel compounds such as ensulizole and febuxostat identified by the cell-based HDAC-Glo assay were selective to HDAC3. Interestingly, nafamostat inhibited HDAC activity more potently in the cell-based HDAC-Glo assays than the isoform-specific HDAC biochemical assays. On the contrary, HDAC inhibition by piceatannol was at least two-fold more potent in the fluorogenic assays of HDAC1, HDAC5, and HDAC8 than the cell-based HDAC-Glo assays (Suppl. **Table S4**). Based on the potency and the efficacy values of the cell-based and biochemical assay data, HDAC8 seems to be the primary target of piceatannol for full inhibition of HDACs in cells and piceatannol also acts as a pan-HDAC inhibitor like its analog resveratrol¹⁶.

To conclude, the qHTS workflow described in this study is useful to rapidly identify compounds that inhibit endogenous HDAC class I and II in physiologically relevant cell backgrounds. We have shown that the HDAC-Glo I/II assay is suitable for primary screening of large chemical libraries in cell lines of interest. Compared to primary screening at a single concentration, the qHTS approach used in the current study has a great advantage in reducing false positive and false negative rates from the primary screening. The secondary assays provide additional mechanistic insights to HDAC functionalities, such as isoform selectivity. Because of the critical roles of HDACs in numerous diseases, we envision that the workflow described in our report will greatly accelerate the speed of drug discovery of HDAC inhibitors for cancer and neurodegenerative diseases.

Supplementary Material

Refer to Web version on PubMed Central for supplementary material.

Acknowledgements

We thank Danielle VanLeer and Paul Shinn for compound management. We thank Yiming Chen, Henry Zhu, and Kevin Kurtz for technical advice and biochemical profiling experiments.

Funding

The author(s) disclosed receipt of the following financial support for the research, authorship, and/or publication of this article: This work was supported by Intramural Research Program of the National Center for Advancing Translational Sciences (NCATS), National Institutes of Health (NIH) and the interagency agreement IAG #NTR 12003 from the National Institute of Environmental Health Sciences/Division of the National Toxicology Program to the NCATS/NIH.

References

1. Berdasco M, Esteller M. Genetic syndromes caused by mutations in epigenetic genes. *Hum Genet.* 2013; 132(4):359–83. [PubMed: 23370504]
2. Chuang DM, et al. Multiple roles of HDAC inhibition in neurodegenerative conditions. *Trends Neurosci.* 2009; 32(11):591–601. [PubMed: 19775759]
3. Marmorstein R. Structure of histone deacetylases: insights into substrate recognition and catalysis. *Structure.* 2001; 9(12):1127–33. [PubMed: 11738039]
4. Falkenberg KJ, Johnstone RW. Histone deacetylases and their inhibitors in cancer, neurological diseases and immune disorders. *Nat Rev Drug Discov.* 2014; 13(9):673–91. [PubMed: 25131830]
5. West AC, Johnstone RW. New and emerging HDAC inhibitors for cancer treatment. *J Clin Invest.* 2014; 124(1):30–9. [PubMed: 24382387]

6. Halley F, et al. A bioluminogenic HDAC activity assay: validation and screening. *J Biomol Screen*. 2011; 16(10):1227–35. [PubMed: 21832257]
7. Riester D, et al. Non-isotopic dual parameter competition assay suitable for high-throughput screening of histone deacetylases. *Bioorg Med Chem Lett*. 2009; 19(13):3651–6. [PubMed: 19457659]
8. Mazitschek R, et al. Development of a fluorescence polarization based assay for histone deacetylase ligand discovery. *Bioorg Med Chem Lett*. 2008; 18(9):2809–12. [PubMed: 18430569]
9. Riester D, et al. Histone deacetylase inhibitor assay based on fluorescence resonance energy transfer. *Anal Biochem*. 2007; 362(1):136–41. [PubMed: 17250798]
10. Wegener D, et al. Improved fluorogenic histone deacetylase assay for high-throughput- screening applications. *Anal Biochem*. 2003; 321(2):202–8. [PubMed: 14511685]
11. Padige G, et al. Development of an ELISA-Based HDAC Activity Assay for Characterization of Isoform-Selective Inhibitors. *J Biomol Screen*. 2015
12. Ito A, et al. p300/CBP-mediated p53 acetylation is commonly induced by p53-activating agents and inhibited by MDM2. *Embo J*. 2001; 20(6):1331–40. [PubMed: 11250899]
13. Ito A, et al. MDM2-HDAC1-mediated deacetylation of p53 is required for its degradation. *Embo J*. 2002; 21(22):6236–45. [PubMed: 12426395]
14. Barlev NA, et al. Acetylation of p53 activates transcription through recruitment of coactivators/ histone acetyltransferases. *Mol Cell*. 2001; 8(6):1243–54. [PubMed: 11779500]
15. Mottamal M, et al. Histone deacetylase inhibitors in clinical studies as templates for new anticancer agents. *Molecules*. 2015; 20(3):3898–941. [PubMed: 25738536]
16. Venturelli S, et al. Resveratrol as a pan-HDAC inhibitor alters the acetylation status of histone [corrected] proteins in human-derived hepatoblastoma cells. *PLoS One*. 2013; 8(8):e73097. [PubMed: 24023672]

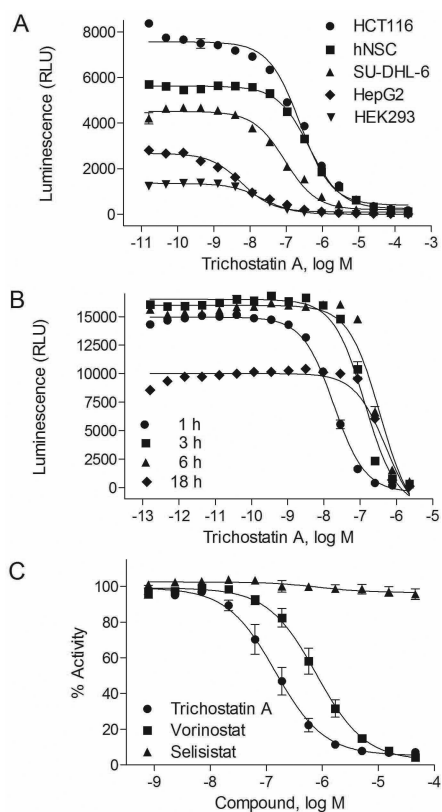


Figure 1. Optimization and validation of the histone deacetylase (HDAC)-Glo I/II assay in 1536-well format

A. Optimal concentration titration of HDAC-Glo I/II activity in HCT116 (average IC_{50} of 0.25 μ M), HEK293 (average IC_{50} of 0.09 μ M), HepG2 (average IC_{50} of 0.05 μ M), human neural stem cells (hNSC) (average IC_{50} of 0.44 μ M), and SU-DHL-6 (average IC_{50} of 0.10 μ M) treated with trichostatin A. **B.** Time course of HDAC-Glo I/II activity in HCT116 cells after treatment of trichostatin A, with average IC_{50} s of 0.02 μ M for 1 hour, 0.11 μ M for 3 hours, 0.22 μ M for 6 hours, and 0.29 μ M for 18 hours, respectively. **C.** Assay selectivity as shown as concentration-response curves of HCT116 cells treated with two known HDAC inhibitors (average IC_{50} s of 0.77 μ M for vorinostat/suberoylanilide hydroxamic acid (SAHA) and 0.07 μ M for trichostatin A) and a sirtuin (SIRT) inhibitor (selisistat, inactive). Each data point was presented as mean \pm SEM from three replicates.

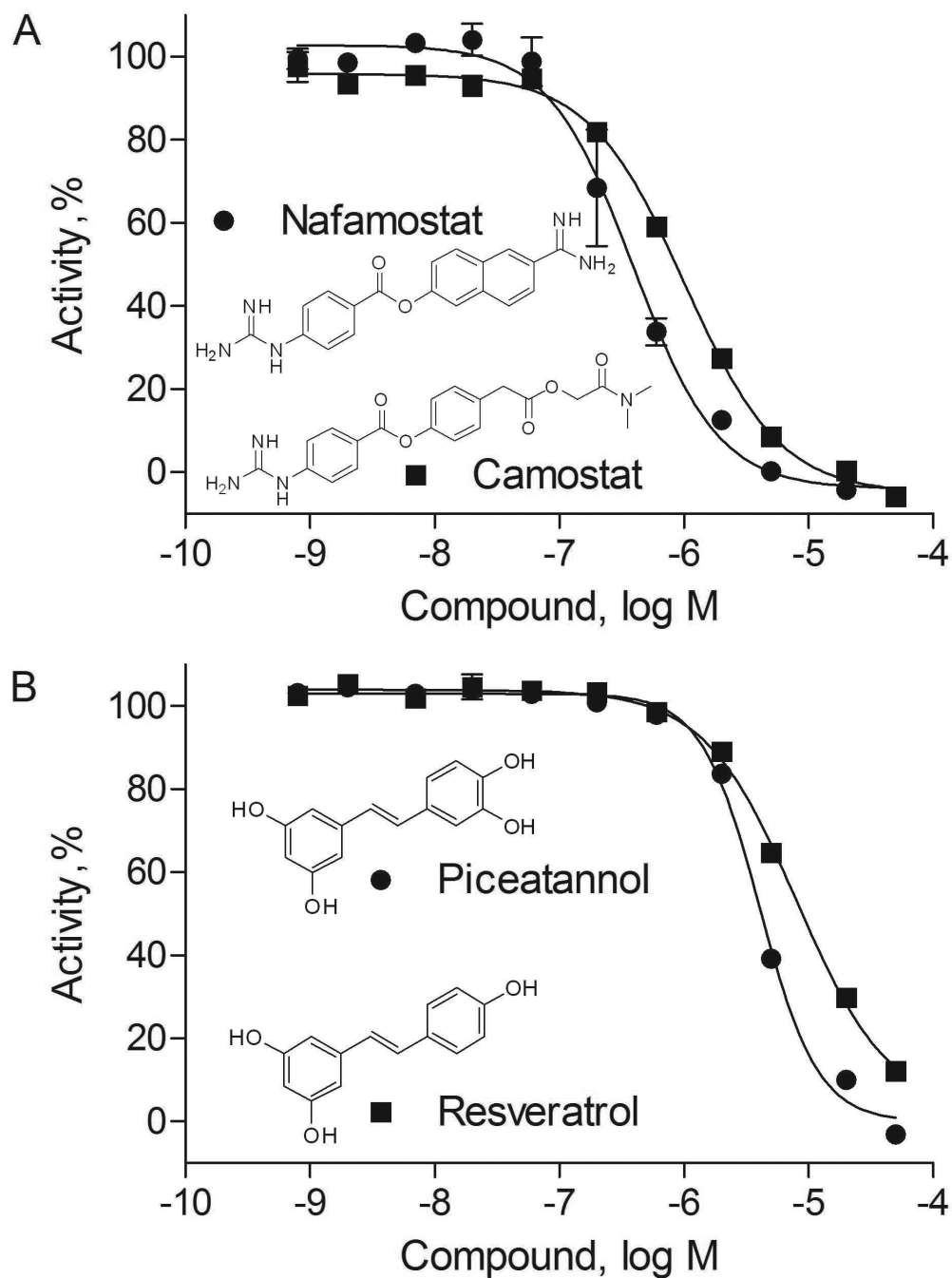


Figure 2. Histone deacetylase (HDAC) inhibitor hits identified from National Center for Advancing Translational Sciences (NCATS) Pharmaceutical Collection

A. Concentration-response curves and chemical structures of nafamostat (average IC_{50} of 0.36 μ M) and camostat (average IC_{50} of 0.95 μ M). **B.** Concentration-response curves and chemical structures of piceatannol (average IC_{50} of 4.18 μ M) and resveratrol (average IC_{50} of 7.43 μ M). Each data point in the concentration-response curves was measured in human neural stem cells (hNSCs) and presented as mean \pm SD from three replicates.

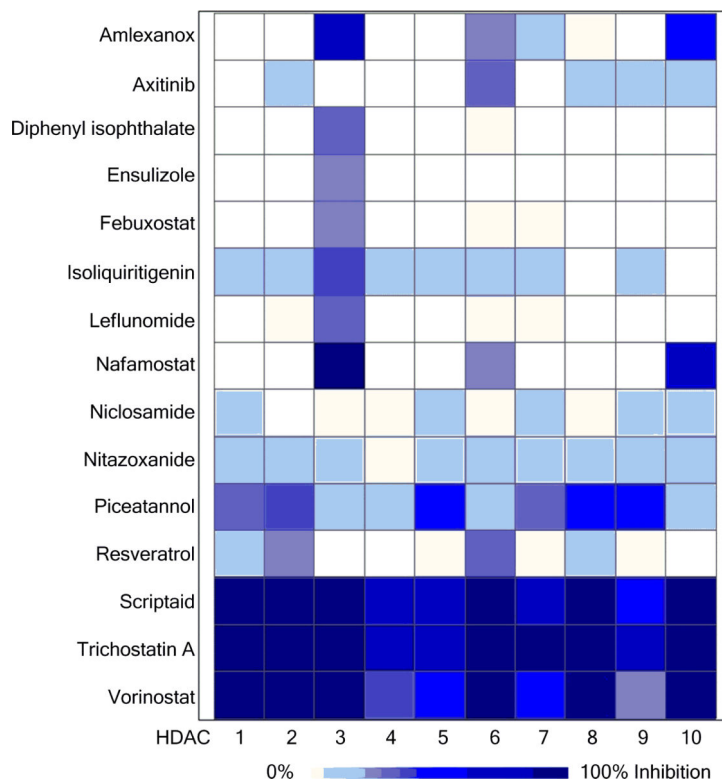


Figure 3. Biochemical profiling of isoform selectivity of histone deacetylase (HDAC) inhibitor hits

In total, 20 μ M of the 15 selected potential HDAC inhibitors were tested with individual recombinant HDAC class I and II enzymes and their corresponding fluorogenic substrates. Efficacy values were averaged from three replicates and shown in heat map.

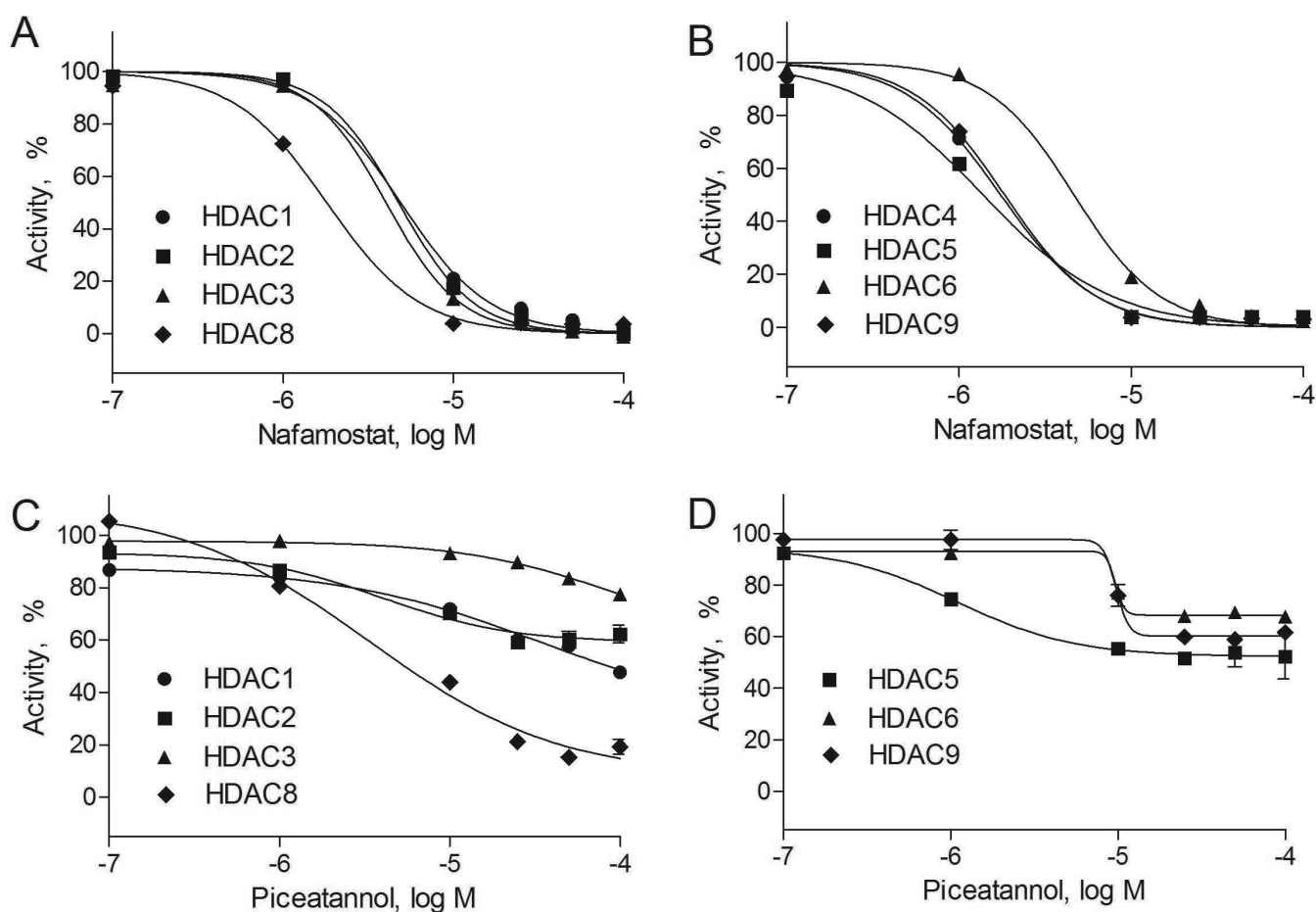


Figure 4. Confirmation of nafamostat and piceatannol identified by both cell-based and biochemical-based Histone deacetylase (HDAC) assays

A. Concentration-response curves of nafamostat in HDAC class I assays (average IC_{50} s of 4.67 μ M for HDAC1, 4.69 μ M for HDAC2, 4.04 μ M for HDAC3, and 1.52 μ M for HDAC8, respectively). **B.** Concentration-response curves of nafamostat in HDAC class II assays (average IC_{50} s of 1.49 μ M for HDAC4, 1.33 μ M for HDAC5, 4.39 μ M for HDAC6, and 1.55 μ M for HDAC9, respectively). **C.** Concentration-response curves of piceatannol in HDAC class I assays (average IC_{50} s of 4.28 μ M for HDAC1, 5.04 μ M for HDAC2, 23.29 μ M for HDAC3, and 3.42 μ M for HDAC8, respectively). **D.** Concentration-response curves of piceatannol in HDAC class II assays. Each data point was presented as mean \pm SD from three replicates (IC_{50} s of 0.89 μ M for HDAC5, 8.22 μ M for HDAC6, and 9.95 μ M for HDAC9, respectively).

Table 1

Cherry-pick confirmation data of the top 20 potential HDAC inhibitors.

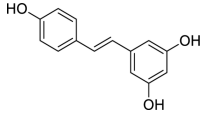
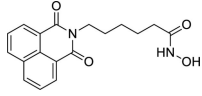
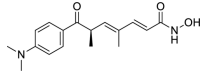
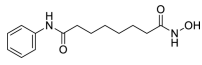
Compound	HDAC-Glo: IC ₅₀ , μM (Efficacy, %)		Viability: IC ₅₀ , μM (Efficacy, %)		Primary target
	hNSC	HCT116	hNSC	HCT116	
Amlexanox	1.10 ± 0.14 (96 ± 7)	1.09 ± 0.07 (110 ± 2)	Inactive	Inactive	TBK1 and IKKε
AR-42	0.76 ± 0.17 (115 ± 5)	0.94 ± 0.11 (113 ± 2)	Inactive	Inactive	HDAC I/II
Ataluren (PTC-124)	0.80 ± 0.05 (109 ± 3)	0.83 ± 0.00 (111 ± 4)	14.28 ± 0.93 (86 ± 10)	14.40 ± 2.45 (103 ± 21)	Ribosome
Axitinib	6.65 ± 0.76 (106 ± 4)	2.97 ± 0.34 (105 ± 3)	26.82 ± 6.13 (27 ± 1)	26.73 ± 10.30 (47 ± 11)	VEGFR1-3, c-KIT, and PDGFRs
Camostat	0.95 ± 0.20 (102 ± 3)	1.94 ± 0.66 (109 ± 4)	Inactive	Inactive	Serine protease
Diphenyl isophthalate	2.24 ± 0.15 (103 ± 3)	3.87 ± 0.81 (112 ± 5)	Inactive	Inactive	Unknown
Ensulizole	1.94 ± 0.97 (111 ± 1)	6.13 ± 3.06 (116 ± 5)	16.02 ± 1.04 (58 ± 5)	13.39 ± 2.80 (70 ± 7)	Unknown
Febuxostat	2.16 ± 0.60 (116 ± 3)	2.38 ± 0.44 (127 ± 5)	Inactive	Inactive	Xanthine oxidase
Isoliquritigenin	2.02 ± 0.13 (117 ± 5)	1.67 ± 0.19 (110 ± 3)	Inactive	Inactive	SIRT activator.
ISOX	1.96 ± 0.35 (118 ± 6)	2.32 ± 0.65 (124 ± 5)	Inactive	Inactive	HDAC I/II
Leflunomide	5.90 ± 0.00 (106 ± 2)	9.48 ± 1.98 (118 ± 11)	Inactive	Inactive	DHODH
Nafamostat	0.36 ± 0.14 (108 ± 1)	1.11 ± 0.25 (116 ± 3)	Inactive	Inactive	Serine protease
Niclosamide	1.40 ± 0.24 (102 ± 4)	2.38 ± 0.16 (112 ± 2)	Inactive	Inactive	Unknown
Nitazoxanide	1.05 ± 0.12 (104 ± 1)	1.60 ± 0.10 (116 ± 1)	12.42 ± 4.65 (40 ± 8)	23.56 ± 11.98 (62 ± 6)	PFOR
Piceatannol	4.18 ± 0.00 (108 ± 4)	5.90 ± 0.00 (105 ± 7)	19.50 ± 2.49 (25 ± 7)	Inactive	SIRT1 and Syk
Pracinostat	0.27 ± 0.06 (112 ± 5)	0.35 ± 0.06 (114 ± 4)	Inactive	Inactive	HDAC I/II
Resveratrol	7.43 ± 0.00 (102 ± 4)	11.02 ± 1.98 (97 ± 13)	Inactive	Inactive	SIRTs and HDAC I/II
Scriptaid	1.19 ± 0.25 (113 ± 6)	1.87 ± 0.22 (123 ± 3)	Inactive	Inactive	HDAC I/II
Trichostatin A	0.10 ± 0.02 (114 ± 6)	0.07 ± 0.01 (119 ± 5)	Inactive	Inactive	HDAC I/II
Vorinostat	0.66 ± 0.08 (101 ± 2)	0.77 ± 0.05 (119 ± 6)	Inactive	Inactive	HDAC I/II

Data were represented as mean ± SD from three replicates. DHODH: dihydroorotate dehydrogenase; HDAC, histone deacetylase; hNSC, human neural stem cell; IKKε: IκB kinase ε. PDGFRs: Platelet-derived growth factor receptors. PFOR: pyruvate/ferredoxin oxidoreductase. TBK1: TANK-binding kinase 1. VEGFR1-3: vascular endothelial growth factor receptor 1-3.

Table 2

Powder confirmation data of the 15 selected compounds in the HDAC-Glo I/II HCT116 assay.

Compound Name (CASRN)	Chemical Structure	IC ₅₀ , μ M (Efficacy, %)
Amlexanox (68302-57-8)		1.65 \pm 0.36 (98 \pm 0)
Axitinib (319460-85-0)		7.83 \pm 0.41 (78 \pm 1)
Diphenyl isophthalate (744-45-6)		5.28 \pm 0.63 (97 \pm 0)
Ensulizole (27503-81-7)		1.66 \pm 0.73 (98 \pm 0)
Febuxostat (144060-53-7)		2.43 \pm 0.27 (96 \pm 1)
Isoliquiritigenin (961-29-5)		2.36 \pm 0.11 (97 \pm 0)
Leflunomide (75706-12-6)		5.61 \pm 0.12 (92 \pm 0)
Nafamostat (82956-11-4)		0.12 \pm 0.03 (99 \pm 0)
Niclosamide (50-65-7)		2.08 \pm 0.17 (98 \pm 1)
Nitazoxanide (55981-09-4)		1.35 \pm 0.14 (99 \pm 0)
Piceatannol (10083-24-6)		10.33 \pm 1.06 (60 \pm 4)

Compound Name (CASRN)	Chemical Structure	IC ₅₀ , μM (Efficacy, %)
Resveratrol (501-36-0)		18.20 ± 2.05 (69 ± 2)
Scriptaid (287383059-9)		1.76 ± 0.24 (93 ± 1)
Trichostatin A (58880-19-6)		0.11 ± 0.01 (99 ± 0)
Vorinostat (149647-78-9)		0.45 ± 0.04 (99 ± 0)

Data are represented as mean ± SD from three replicates. HDAC, histone deacetylase

Author Manuscript

Author Manuscript

Author Manuscript

Author Manuscript